Rational Design of Quasi Zero-Strain NCM Cathode Materials for Minimizing Volume Change Effects in All-Solid-State Batteries

Florian Strauss,*,† Lea de Biasi,† A-Young Kim,† Jonas Hertle,‡ Simon Schweidler,† Jürgen Janek,†,‡ Pascal Hartmann,*,†,§ and Torsten Brezesinski*,†

†Battery and Electrochemistry Laboratory, Institute of Nanotechnology, Karlsruhe Institute of Technology (KIT), Hermann-von-Helmholtz-Platz 1, 76344 Eggenstein-Leopoldshafen, Germany

‡Institute of Physical Chemistry & Center for Materials Science, Justus-Liebig-University Giessen, Heinrich-Buff-Ring 17, 35392 Giessen, Germany

§BASF SE, Carl-Bosch-Strasse 38, 67056 Ludwigshafen, Germany

ABSTRACT: Measures to improve the cycling performance and stability of bulk-type all-solid-state batteries (SSBs) are currently being developed with the goal of substituting conventional Li-ion battery (LIB) technology. As known from liquid electrolyte-based LIBs, layered oxide cathode materials undergo volume changes upon (de)lithiation, causing mechanical degradation because of particle fracture, among others. Unlike solid electrolytes, liquid electrolytes are somewhat capable of accommodating morphological changes. In SSBs, the rigidity of the materials used typically leads to adverse contact loss at the interfaces of cathode material and solid electrolyte during cycling. Hence, designing zero- or low-strain electrode materials for application in next-generation SSBs is desirable. In the present work, we report on novel Co-rich NCMs, NCM361 (60% Co) and NCM271 (70% Co), showing minor volume changes up to 4.5 V versus Li^+/Li, as determined by *operando* X-ray diffraction and pressure measurements of LIB pouch and pelletized SSB cells, respectively. Both cathode materials exhibit good cycling performance when incorporated into SSB cells using argyrodite Li_6PS_5Cl solid electrolyte, albeit their morphology and secondary particle size have not yet been optimized.

Solidifying LIBs by substituting the liquid organic electrolyte by a solid Li-ion conductor is considered a promising approach toward inherently safe batteries with enhanced energy and power densities.[1,2] Implementation of layered oxides at the cathode side, such as $Li_{1+x}(Ni_{1-y-z}Co_yMn_z)_{1-x}O_2$ (referred to as NCM or NMC), seems necessary to be able to compete with state-of-the-art LIBs.[3-5] However, bulk-type SSB cells usually exhibit lower performance than conventional LIB cells for the same NCM. This is due in part to interfacial instability between the cathode active material (CAM) and the solid electrolyte (SE) during cycling and in part to chemomechanical degradation because of NCM "breathing" upon (de)lithiation (referring to unit cell volume changes).[6–12] Note that for the same cutoff voltage on charge, the absolute relative volume change increases with increasing Ni content.[6,9] While the lattice contraction and expansion of especially Ni-rich NCMs have been shown to contribute to capacity fading in liquid electrolyte-based LIBs,[10] such intrinsic volume effects are much more detrimental to the performance of SSBs [because of the rigidity (hardness) of the materials used].[11,12] Hence, application of electrode materials showing negligible volume changes with cycling would certainly be favorable. However, rational design of reduced-strain NCM CAMs remains elusive so far. Nonetheless, there is a theoretical study proposing prototype materials of general formula LiM_2O_4, with M being a mixture of Mn, Mg, and Cr, exhibiting zero- or low-strain properties.[13]

In order to provide fundamental design principles for quasi zero-strain layered oxide CAMs, the molar ratio of Co/(Ni+Co) versus the relative change in unit cell volume for different cutoff voltages of 4.3, 4.4, and 4.6 V with respect to Li^+/Li has been plotted and analyzed (**Figures 1** and **S1**). Because Mn can be considered electrochemically inactive, it has not been taken into account.[14,15] As can be seen, the relative volume changes vary—depending on the cutoff voltage—from about −7% to +2% for Ni- and Co-rich phases, respectively.

Next, linear curve fitting has been done to the available data points to reveal the Co content that may lead to zero-strain behavior. The shaded area around 0% relative volume change in **Figure 1** indicates that the molar ratio of Co/(Ni+Co) should be about 70% for a cutoff voltage of 4.4 V versus Li^+/Li. Based on this insight, two Co-rich CAMs, namely NCM361 (60% Co) and NCM271 (70% Co), have been synthesized for application in SSB cells.

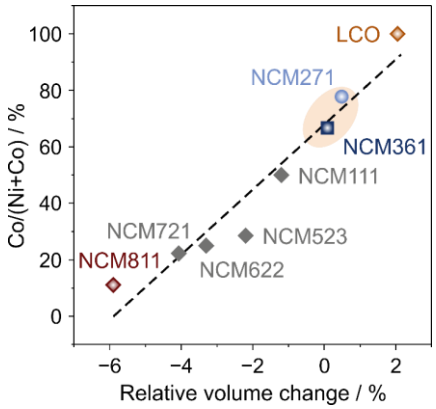

Figure 1. Molar ratio of Co/(Ni+Co) versus the relative change in unit cell volume for various layered oxide cathode active materials (from *operando* X-ray diffraction of LIB pouch cells charged to 4.4 V vs Li^+/Li). The dashed line is a linear fit to the experimental data. Note that LCO refers to $LiCoO_2$.

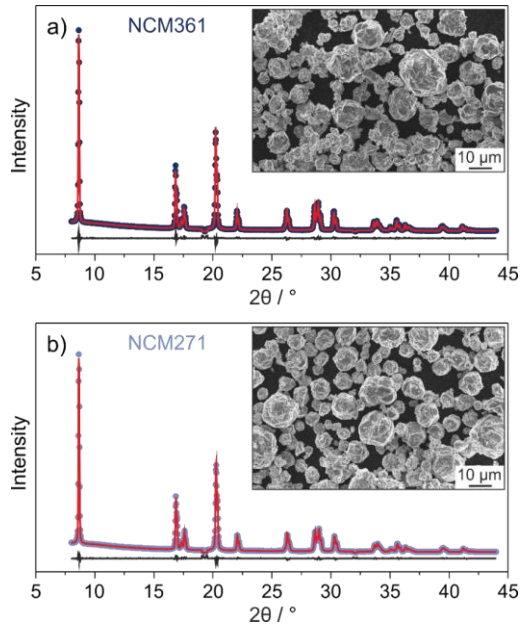

Figure 2. Rietveld refinement analysis of *ex situ* X-ray diffraction data obtained on pristine (a) NCM361 and (b) NCM271. Measured patterns are in dark and pale blue, calculated patterns in orange, with R_{wp} being 3.73 and 3.29, respectively, and difference profiles in black. Insets are low-magnification scanning electron microscopy images.

They adopt the α-$NaFeO_2$ structure (*R*–3m space group), characteristic of layered NCMs, and the micrometer-sized secondary particles are of spherical shape according to scanning electron microscopy imaging (**Figure 2**).[6] They also seem to be fairly stable under ambient (laboratory) conditions, which may facilitate storage and handling. Lattice parameters from Rietveld refinement analysis of *ex situ* X-ray diffraction data are provided in **Table 1**. An increase in lattice parameter *a* with increasing Ni content is noticed because of the larger ionic radii of Ni^{2+} (0.69 Å) and Ni^{3+} (0.56 Å) than Co^{3+} (0.55 Å) and Mn^{4+} (0.53 Å). Likewise, the lattice parameter *c* increases, but there is apparently no clear trend with ion size that can account for this result.[6,16]

Table 1. Lattice parameters *a* and *c* and oxygen *z* position for pristine NCM361 and NCM271.

Sample	*a* / Å	*c* / Å	*z*
NCM361	2.8411(7)	14.1464(1)	0.2397(9)
NCM271	2.8346(2)	14.1307(6)	0.2388(9)

First, both CAMs have been tested electrochemically in liquid electrolyte-based LIB coin cells (details in Supporting Information). As is evident from **Figure S2**, they deliver similar specific discharge capacities at a C/5 rate, which increase from about 160 to 210 mAh/g_{NCM} when increasing the cutoff voltage from 4.3 to 4.6 V versus Li^+/Li. This increase is quite significant and rather comparable to that of LCO than of NCM811 (**Figure S3**). However, as known for layered oxide CAMs, the upper cutoff voltage must be chosen carefully as irreversible structural changes may occur when the battery cell is operated at high states of charge, eventually leading to performance decay.[6,10]

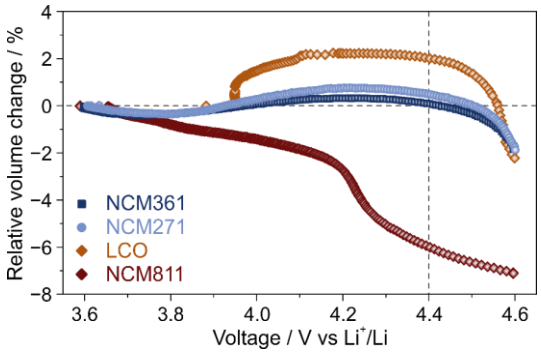

Figure 3. Relative changes in unit cell volume for various layered oxide cathode active materials (from *operando* X-ray diffraction of LIB pouch cells).

In order to determine the most favorable voltage range for NCM361 and NCM271 in terms of structural stability and relative volume change, *operando* X-ray diffraction has been conducted on LIB pouch cells, following an initial formation procedure (details in Supporting Information). As opposed to LCO and NCM811, both CAMs show relative changes in unit cell volume of less than 1% during charge up to 4.5 V versus Li^+/Li (**Figure 3**). However, they exhibit non-negligible volume contraction for higher voltages. Note that the anisotropic changes in lattice parameters—that is, the expansion and contraction along the *c*- and *a*-axis, respectively, up to $x(Li) \approx 0.45$ and then vice versa with further delithiation—largely balance out, so that the net relative volume changes are virtually zero (**Figure 4**). This is also why these materials are referred to as "quasi zero-strain" in the present work. Moreover, the lattice changes during cycling have been found by X-ray diffraction to be reversible (see contour plots and line patterns for NCM361 and NCM271 in **Figures S4** and **S5**, respectively).

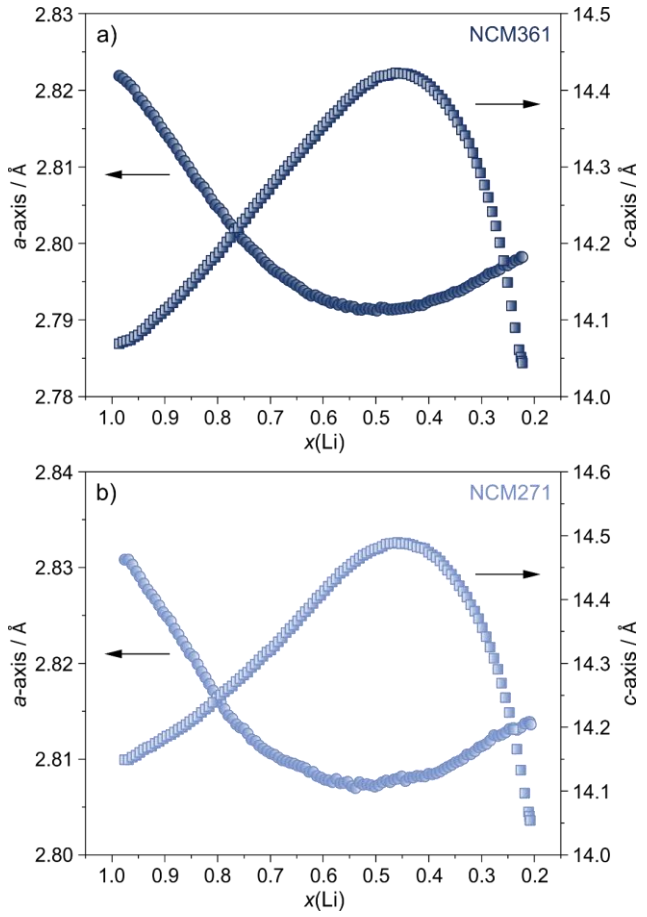

Figure 4. Changes in lattice parameters *a* and c of (a) NCM361 and (b) NCM271 (from *operando* X-ray diffraction of LIB pouch cells charged to 4.6 V vs Li^+/Li).

Subsequently, their cyclability in pelletized SSB cells using argyrodite Li_6PS_5Cl as the SE has been examined. To this end, cathode and anode composites comprising either NCM361 or NCM271 and $Li_4Ti_5O_{12}$ (LTO), respectively, were prepared by ball milling. Prior to their use, a 1 wt.% $LiNbO_3$ protective surface coating was applied to both CAMs by following an established preparation procedure.[17] The electrochemical cycling has been done in customized cells under a steady pressure of 55 MPa (details in Supporting Information) and in the voltage range between 1.35 and 2.85 V with respect to $Li_4Ti_5O_{12}/Li_7Ti_5O_{12}$ (corresponding to about 2.9–4.4 V vs Li^+/Li). The initial voltage profiles at a C/10 rate are shown in **Figure 5a**. First cycle specific charge and discharge capacities of around 170 and 140 mAh/g_{NCM} (~1.5 mAh/cm^2), respectively, were achieved, corresponding to Coulombic efficiencies of 82%, compared to 96% for liquid electrolyte-based LIB cells. The origin of the reduced initial Coulombic efficiency presumably lies in side reactions at the CAM/SE interfaces, indicating that the effect of the $LiNbO_3$ coating is limited. However, SE decomposition at the interfaces with the carbon black additive cannot be ruled out. Besides, the presence of electrically isolated CAM particles and/or electrode sections may help explain the lower attainable specific capacities (note that electrochemical testing has been performed on relatively simple pelletized cells).[18,19]

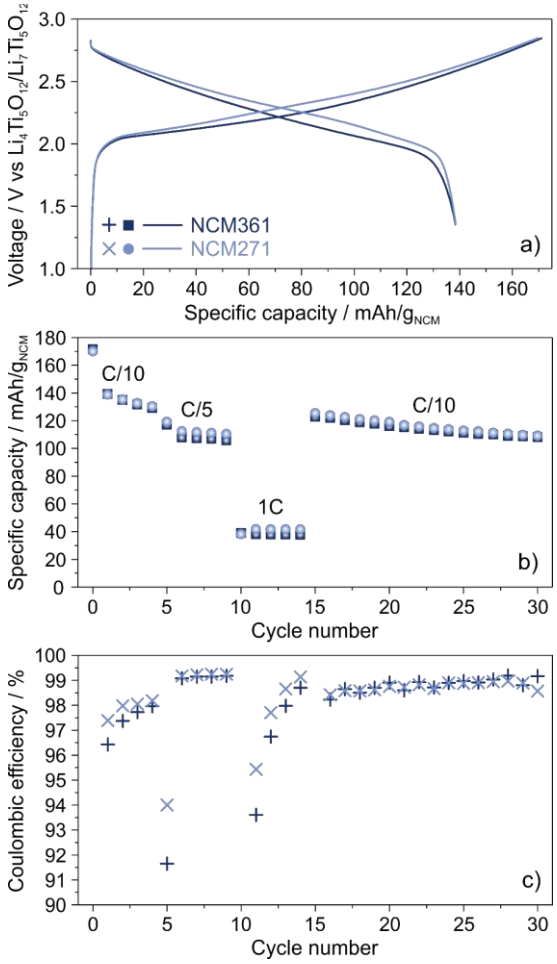

Figure 5. Room-temperature cycling performance of NCM361 and NCM271 in SSB cells. (a) Initial voltage profiles, (b) specific charge capacities for different C-rates, and (c) Coulombic efficiencies over 30 cycles.

As can be also seen from **Figure 5a**, NCM361 exhibits a lower mean charge/discharge voltage than NCM271, which seems to be due to the slightly lower operating voltage of Ni redox (compared to Co redox). With further cycling, the capacity decay slows down (**Figure 5b**), and the Coulombic efficiency increases to 98% over the first 5 cycles (**Figure 5c**). After 30 cycles, the SBB cells are still capable of delivering specific capacities of about 110 mAh/g_{NCM}, with the Coulombic efficiency approaching 99%. The fading is certainly in part because of the ill-defined nature and non-uniformity of the sol-gel-derived coating, leading to continuous SE decomposition, that is, during the later cycles as well, albeit less severe. For the same reason, the coating is also not expected to have any effect on the CAMs' bulk properties.[20]

In recent years, it has been shown that the interfacial degradation processes involve chemical changes, such as S–S, S–O, and P–S–P bond formation (independent of the CAM composition). Likewise, PO_x species have been observed by X-ray photoelectron spectroscopy and time-of-flight secondary-ion mass spectrometry.[21,22] SE decomposition also negatively affects the interfacial charge transfer kinetics, as is evident from the low cell capacities achieved at a 1C rate. However, considering that the

electrode materials themselves and the coating chemistry have not yet been optimized, the cycling performance, which is virtually identical for both CAMs, is promising.[18]

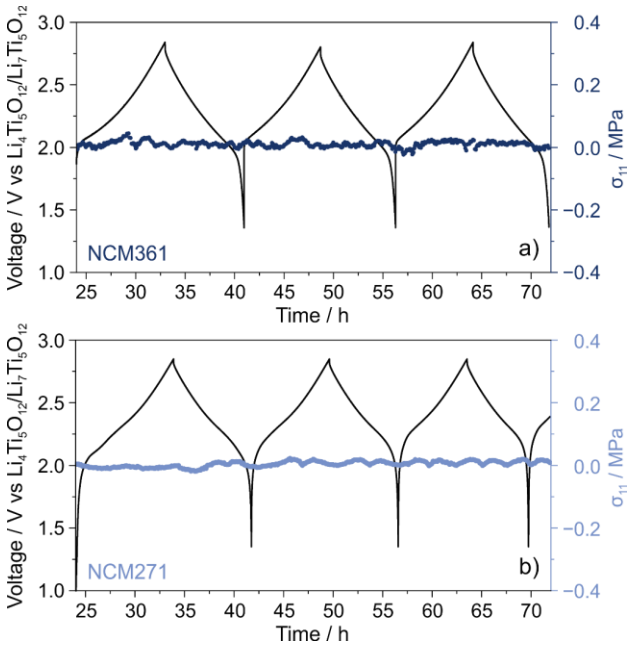

Figure 6. Background-corrected net stress of SSB cells using (a) NCM361 and (b) NCM271 and the corresponding voltages profiles.

As mentioned above, mechanical separation between the CAM and SE particles may give rise to performance degradation. One way to track down such problems is to monitor the pressure (stress) evolution.[12] Here, pressure changes in operating SSB cells using NCM361 or NCM271 have been measured *in situ* using a customized setup (details in Supporting Information). The corresponding time-resolved and background-corrected data are shown in **Figure 6**, indicating no significant changes in linear elastic stress (σ_{11}) during the course of cycling [i.e., there is virtually no x(Li) dependence]. This result is in agreement with the relative volume changes ($\Delta V/V_0 << 1\%$) determined by comparing the (estimated) degree of delithiation of NCM361 and NCM271 in SSB cells with that achieved in LIB pouch cells (**Figure S6**).[19] It is also important to note that the absolute relative volume changes of NCM811 and LCO are much larger for the same degree of delithiation. However, although the net stress data are rather featureless, chemomechanically driven phase separation cannot be fully ruled out because of the anisotropic changes in lattice parameters.[7,10]

In summary, we have successfully designed—in a rational manner—novel Co-rich NCMs for application in SSBs. These cathode active materials showed minor volume changes upon (de)lithiation, as confirmed by *operando* X-ray diffraction and pressure measurements. For SSBs, in particular, the use of zero- or low-strain (active) materials is favorable to prevent gap formation between the solid electrolyte and ion storage particles during operation. Notably, bulk-type cells using electrodes of practical loading exhibited good cycling performance at room temperature, despite the fact that the secondary particle size and electrode composition have not yet been optimized. Nonetheless, the question remains whether such quasi zero-strain Co-rich NCMs are superior to state-of-the-art Ni-rich NCMs in terms of cyclability and stability.

Taken together, this study presents a unique strategy to tailor layered oxide cathode active materials for SSB applications by considering volume change effects on both the atomic (unit cell level) and macro (electrode level) scales.

ASSOCIATED CONTENT

Experimental details regarding materials preparation, cell assembly, and structural/electrochemical characterization; contour plots and line patterns of *operando* XRD data; additional electrochemical testing results and unit cell volume change data. This material is available free of charge via the Internet at http://pubs.acs.org

AUTHOR INFORMATION

Corresponding Authors

*E-mail: florian.strauss@kit.edu; Phone: +49 721 60828907.
*E-mail: pascal.hartmann@basf.com; Phone: +49 621 6048636.
*E-Mail: torsten.brezesinski@kit.edu; Phone: +49 721 60828827.

ORCID

Florian Strauss: 0000-0001-5817-6349
Lea de Biasi: 0000-0001-8546-0388
A-Young Kim: 0000-0001-6124-0807
Simon Schweidler: 0000-0003-4675-1072
Jürgen Janek: 0000-0002-9221-4756
Torsten Brezesinski: 0000-0002-4336-263X

Present Address

L.d.B.: Institute for Applied Materials–Energy Storage Systems, Karlsruhe Institute of Technology (KIT), Eggenstein-Leopoldshafen, Germany
A.-Y.K.: Mercedes-Benz Korea Ltd., Seoul, Republic of Korea

Notes

The authors declare no competing financial interest.

ACKNOWLEDGMENT

This study is part of the projects being funded within the BASF International Network for Batteries and Electrochemistry.

REFERENCES

(1) Janek, J.; Zeier, W. G. A Solid Future for Battery Development. *Nat. Energy* **2016**, *1*, 16141.
(2) Kerman, K.; Luntz, A.; Viswanathan, V.; Chiang, Y.-M.; Chen, Z. Review—Practical Challenges Hindering the Development of Solid State Li Ion Batteries. *J. Electrochem. Soc.* **2017**, *164*, A1731–A1744.
(3) Myung, S.-T.; Maglia, F.; Park, K.-J.; Yoon, C. S.; Lamp, P.; Kim, S.-J.; Sun, Y.-K. Nickel-Rich Layered Cathode Materials for Automotive Lithium-Ion Batteries: Achievements and Perspectives. *ACS Energy Lett.* **2017**, *2*, 196–223.
(4) Bianchini, M.; Roca-Ayats, M.; Hartmann, P.; Brezesinski, T.; Janek, J. There and Back Again—The Journey of $LiNiO_2$ as a Cathode Active Material. *Angew. Chem. Int. Ed.* **2019**, *58*, 10434–10458.

(5) Sun, Y.-K. High-Capacity Layered Cathodes for Next-Generation Electric Vehicles. *ACS Energy Lett.* **2019**, *4*, 1042–1044.

(6) de Biasi, L.; Kondrakov, A. O.; Geßwein, H.; Brezesinski, T.; Hartmann, P.; Janek, J. Between Scylla and Charybdis: Balancing Among Structural Stability and Energy Density of Layered NCM Cathode Materials for Advanced Lithium-Ion Batteries. *J. Phys. Chem. C* **2017**, *121*, 26163–26171.

(7) Kondrakov, A. O.; Schmidt, A.; Xu, J.; Geßwein, H.; Mönig, R.; Hartmann, P.; Sommer, H.; Brezesinski, T.; Janek, J. Anisotropic Lattice Strain and Mechanical Degradation of High- and Low-Nickel NCM Cathode Materials for Li-Ion Batteries. *J. Phys. Chem. C* **2017**, *121*, 3286–3294.

(8) Lim, J.-M.; Hwang, T.; Kim, D.; Park, M.-S.; Cho, K.; Cho, M. Intrinsic Origins of Crack Generation in Ni-rich $LiNi_{0.8}Co_{0.1}Mn_{0.1}O_2$ Layered Oxide Cathode Material. *Sci. Rep.* **2017**, *7*, 39669.

(9) Ishidzu, K.; Oka, Y.; Nakamura, T. Lattice Volume Change during Charge/Discharge Reaction and Cycle Performance of $Li[Ni_xCo_yMn_z]O_2$. *Solid State Ionics* **2016**, *288*, 176–179.

(10) Ryu, H.-H.; Park, K.-J.; Yoon, C. S.; Sun, Y.-K. Capacity Fading of Ni-Rich $Li[Ni_xCo_yMn_{1-x-y}]O_2$ ($0.6 \le x \le 0.95$) Cathodes for High-Energy-Density Lithium-Ion Batteries: Bulk or Surface Degradation? *Chem. Mater.* **2018**, *30*, 1155–1163.

(11) Koerver, R.; Aygün, I.; Leichtweiß, T.; Dietrich, C.; Zhang, W.; Binder, J. O.; Hartmann, P.; Zeier, W. G.; Janek, J. Capacity Fade in Solid-State Batteries: Interphase Formation and Chemomechanical Processes in Nickel-Rich Layered Oxide Cathodes and Lithium Thiophosphate Solid Electrolytes. *Chem. Mater.* **2017**, *29*, 5574–5582.

(12) Koerver, R.; Zhang, W.; de Biasi, L.; Schweidler, S.; Kondrakov, A. O.; Kolling, S.; Brezesinski, T.; Hartmann, P.; Zeier, W. G.; Janek, J. Chemo-Mechanical Expansion of Lithium Electrode Materials – On the Route to Mechanically Optimized All-Solid-State Batteries. *Energy Environ. Sci.* **2018**, *11*, 2142–2158.

(13) Rosciano, F.; Christensen, M.; Eyert, V.; Mavromaras, A.; Wimmer, E. Reduced Strain Cathode Materials for Solid State Lithium Ion Batteries. WO/2014/191018.

(14) Kondrakov, A. O.; Geßwein, H.; Galdina, K.; de Biasi, L.; Meded, V.; Filatova, E. O.; Schumacher, G.; Wenzel, W.; Hartmann, P.; Brezesinski, T.; et al. Charge-Transfer-Induced Lattice Collapse in Ni-Rich NCM Cathode Materials during Delithiation. *J. Phys. Chem. C* **2017**, *121*, 24381–24388.

(15) Cherkashinin, G.; Motzko, M.; Schulz, N.; Späth, T.; Jaegermann, W. Electron Spectroscopy Study of $Li[Ni,Co,Mn]O_2$/Electrolyte Interface: Electronic Structure, Interface Composition, and Device Implications. *Chem. Mater.* **2015**, *27*, 2875–2887.

(16) Shannon, R. D. Revised Effective Ionic Radii and Systematic Studies of Interatomic Distances in Halides and Chalcogenides. *Acta Crystallogr. A* **1976**, *32*, 751–767.

(17) Oh, G.; Hirayama, M.; Kwon, O.; Suzuki, K.; Kanno, R. Bulk-Type All Solid-State Batteries with 5 V Class $LiNi_{0.5}Mn_{1.5}O_4$ Cathode and $Li_{10}GeP_2S_{12}$ Solid Electrolyte. *Chem. Mater.* **2016**, *28*, 2634–2640.

(18) Strauss, F.; Bartsch, T.; de Biasi, L.; Kim, A.-Y.; Janek, J.; Hartmann, P.; Brezesinski, T. Impact of Cathode Material Particle Size on the Capacity of Bulk-Type All-Solid-State Batteries. *ACS Energy Lett.* **2018**, *3*, 992–996.

(19) Bartsch, T.; Kim, A.-Y.; Strauss, F.; de Biasi, L.; Teo, J. H.; Janek, J.; Hartmann, P.; Brezesinski, T. Indirect State-of-Charge Determination of All-Solid-State Battery Cells by X-Ray Diffraction. *Chem. Commun.* **2019**, *55*, 11223–11226.

(20) Neudeck, S.; Mazilkin, A.; Reitz, C.; Hartmann, P.; Janek, J.; Brezesinski, T. Effect of Low-Temperature Al_2O_3 ALD Coating on Ni-Rich Layered Oxide Composite Cathode on the Long-Term Cycling Performance of Lithium-Ion Batteries. *Sci. Rep.* **2019**, *9*, 5328.

(21) Walther, F.; Koerver, R.; Fuchs, T.; Ohno, S.; Sann, J.; Rohnke, M.; Zeier, W. G.; Janek, J. Visualization of the Interfacial Decomposition of Composite Cathodes in Argyrodite-Based All-Solid-State Batteries Using Time-of-Flight Secondary-Ion Mass Spectrometry. *Chem. Mater.* **2019**, *31*, 3745–3755.

(22) Auvergniot, J.; Cassel, A.; Ledeuil, J.-B.; Viallet, V.; Seznec, V.; Dedryvère, R. Interface Stability of Argyrodite Li_6PS_5Cl toward $LiCoO_2$, $LiNi_{1/3}Co_{1/3}Mn_{1/3}O_2$, and $LiMn_2O_4$ in Bulk All-Solid-State Batteries. *Chem. Mater.* **2017**, *29*, 3883–3890.

TOC GRAPHIC

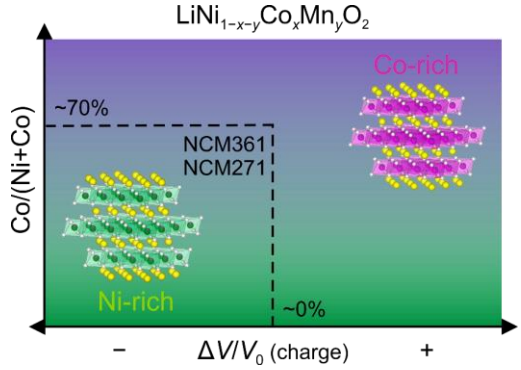
LiNi1−x−yCoxMnyO2
Co-rich
~70%
NCM361
NCM271
Co/(Ni+Co)
Ni-rich
~0%
−
ΔV/V0 (charge)
+